ACS OMEGA

Open Access

http://pubs.acs.org/journal/acsodf

Article

Comparative Study on Morphological Features and Chemical Components of Wild and Cultivated *Angelica sinensis* Based on Bionic Technologies and Chemometrics

Yiyang Chen, Jialing Zhang, Juanjuan Liu, Huifang Hu, Liangcai Wang, and Ling Jin*

Cite This: *ACS Omega* 2024, 9, 41408−41418

Read Online

ACCESS | Metrics & More | Article Recommendations | Supporting Information

ABSTRACT: As a traditional Chinese medicine, *Angelica sinensis* is primarily sourced from cultivated plants due to the significant decline in wild resources. This shift raises concerns about potential differences in efficacy resulting from variations in morphological features and chemical composition between wild (WA) and cultivated (CA) *A. sinensis*. In this study, a suite of advanced analytical techniques including electronic nose, electronic tongue, and electronic eye, alongside headspace solid-phase microextraction coupled with gas chromatography−mass spectrometry and high-performance liquid chromatography, was applied to compare the morphological features and chemical components of WA and CA. Furthermore, principal component analysis and partial least-squares discriminant were employed for data analysis. The morphological features and chemical components of WA and CA were compared and analyzed. The results showed that three bionic technologies can distinguish WA from CA well and that fusion signals can distinguish better. There were differences between WA and CA in odor, taste, color, and content of the indicator components. There were correlations between the morphological features and the content of indicator components.

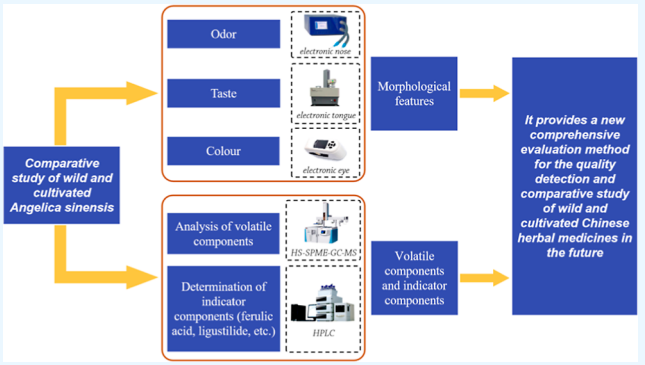

1. INTRODUCTION

Chemical components are the material basis for traditional Chinese medicine (TCM) and exert their efficacy. According to their different growth patterns, TCM can be divided into wild and cultivated forms, both of which are used in clinical practice. In the past, the supply of medicinal plants substantially depended on wild resources. With the rapid evolution of society, however, the impact of human activities on the ecological environment is becoming increasingly intense, leading to significant reduction in the natural habits and reserves of wild resources. The gap between the escalating market demand and the shrinking supply of raw materials has become increasingly prominent. In this case, artificial cultivation of medicinal plants has become one of the most effective measures for addressing such an issue. In fact, most TCMs commonly used in clinical practice have achieved large-scale artificial cultivation, or in other words, the market circulation of TCM has been dominated by the cultivated. However, the morphological features of some cultivated TCM have changed significantly. The change in morphological features also indicates the change in chemical components of TCM, and the efficacy is very likely to change. This has caused concerns about the quality of cultivated TCM.[1,2] Because of the large differences in morphological features of wild and cultivated TCM,[3,4] *the Chinese Pharmacopoeia* (2020) has separated wild and cultivated under some varieties such as Radix Salviae Miltiorrhizae, Radix Codonopsis, and Radix Stellariae. Comparing wild TCM with cultivated TCM, differences and causes in quality will be found, and so the changes in clinical efficacy brought by them, which is of positive significance to explore the alternative use of wild and cultivated TCM.

Angelicae Sinensis Radix is the dried root of *Angelica sinensis* (Oliv.) Diels belonging to the family Apiaceae. It has the effects of replenishing blood and promoting blood circulation, regulating menstruation relieving pain, and cleaning the intestine for relaxing bowels.[5,6] Relevant studies have shown that the distribution of wild (WA) *A. sinensis* resources in China is very sparse, limited to some alpine regions and inaccessible mountain jungles in Gansu, Sichuan, Tibet, Yunnan, and other provinces.[7] In recent years, due to the increasing demand and rising price of *A. sinensis*, farmers in many producing areas have carried out devastating cutting of

Received: May 8, 2024
Revised: September 14, 2024
Accepted: September 19, 2024
Published: September 26, 2024

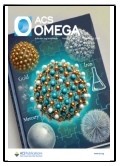

Figure 1. Comparison of morphological features between WA and CA in 15 batches.

WA. In addition, the low germination rate, slow growth, and long growth cycle of WA seeds have caused the resources of WA to decrease sharply. At present, the main source of *A. sinensis* is from cultivation.[8] Blindly replacing wild TCM with domestic TCM without evaluating the quality consistency between the two might change the original dose−response relationship, thus bringing risks to clinical application.[9] Therefore, it is of great significance to compare the morphological features and chemical components of WA and cultivated (CA) *A. sinensis*.

The identification and quality evaluation of TCM have always been carried out by methods of mouth taste, eye observation, nose smell, and hand touch. These mainly rely on the basic sensory functions of human beings. They are easily affected by a variety of external factors and have a strong subjectivity. With the development of modern science and technology, bionic technology as a new quality evaluation method has been gradually applied in the field of TCM. Among them, the electronic nose, electronic tongue, and electronic eye are commonly used analytical devices. The electronic nose, electronic tongue, and electronic eye are, respectively, equipped with gas, liquid, and color sensors to mimic the human smell, taste, and visual systems. They can digitize the subjective sensory functions of human beings, making all kinds of human feelings more accurate, objective, and transferable.[10] Nowadays, many correlational studies have been carried out to describe and evaluate the odor, taste, and color of TCM by electronic nose, electronic tongue, or electronic eye, respectively. However, the quality evaluation of TCM is a comprehensive embodiment of many quality factors. Therefore, the electronic nose, electronic tongue, and electronic eye should be combined to establish a new comprehensive evaluation method for morphological features of WA and CA. Headspace solid-phase microextraction with gas chromatography−mass spectrometry (HS-SPME-GC-MS) combines headspace solid-phase microextraction technology with gas chromatography−mass spectrometry to simplify the sample pretreatment method. It is a fast and sensitive new analytical method having a strong ability to separate volatile components.[11] In recent years, fingerprinting has proved to be a simple and effective way to analyze TCM containing complex natural components.[12] Therefore, in this study, HS-SPME-GC-MS and high-performance liquid chromatography (HPLC) fingerprints were used to analyze and compare the chemical components of WA and CA. This analysis provides fundamental information for the further development and optimization of imitation wild cultivation technology and the breeding of *A. sinensis* with strong resistance and wide adaptability. It is significant for the sustainable utilization of *A. sinensis* resources and the exploration of alternative uses for WA and CA. Additionally, it represents an important scientific endeavor to guide the cultivation of high-quality *A. sinensis* and ensure the safety of its use in medicine.[9]

2. MATERIALS AND METHODS

2.1. Materials and Reagents. Since *A. sinensis* is a kind of genuine regional medical plant in Minxian County, the samples were randomly collected from various townships and surrounding areas of Minxian County, Dingxi City, Gansu Province on September 22, 2023. The habitats of *A. sinensis* in each collection site were similar, with altitudes ranging from 2000 to 2600 m, and the growth years were all two years. Ten batches of CA were collected. Due to the rarity of WA and a series of protections, only five batches of WA were collected. About 5 WA plants and 1−2 kg of CA were collected per area. The collected wild plants were identified in appearances. The stems of the wild plants were found to be erect, purple in color, smooth, and glabrous. The fruits were oval in shape with a pale purple edge. The roots were cylindrical, yellowish brown with branches and fibrous roots. Moreover, they had a strong aroma. In addition, the root microstructures of wild and cultivated plants were compared, as shown in Figure S1. It can be identified as the roots of *A. sinensis* (Oliv.) Diels (Figure 1). For sample collection information, refer to Table S1. The growing environments of WA and CA are shown in Figure 2. The collected fresh samples were dried in shade, and then grounded into fine powder and stored in Ziploc bags at 4 °C for analysis.

The standards, chlorogenic acid, ferulic acid, senkyunolide I, senkyunolide H, coniferyl ferulate, falcarindiol, 3-*n*-butylphthalide, senkyunolide A, ligustilide, 3-butylidenephthalide, and levistilide A were all purchased from Shanghai Yuanye Biotechnology (purity ≥98%). Acetic acid glacial was purchased from the Tianjin Damao Chemical Reagent Factory. Chromatographic-grade methanol was purchased from Beijing Mairuida Technology. NaCl was purchased from the Sinopharm Group. 2-Octanol was purchased from Guangzhou Jiatu Technology.

2.2. Bionic Technology Device and Signal Acquisition. *2.2.1. Electronic Nose Setup and Signal Acquisition.*

https://doi.org/10.1021/acsomega.4c04400
ACS Omega 2024, 9, 41408−41418

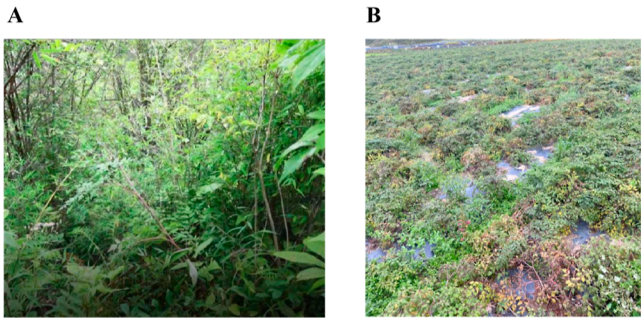

Figure 2. Environments of WA (A) and CA (B).

Approximately 1.0 g of WA and CA powder were weighed and placed into 15 mL headspace vials, which were then sealed tightly with bottle caps. The headspace suction method was applied to the PEN3 electronic nose system (Airsense, Germany). The inlet flow rate was set at 300 mL/min, and the sample was left at room temperature for 5 min to equilibrate. Following this, the sensor underwent a self-cleaning process for 60 s before initiating analysis and sampling, which lasted 150 s. Each sample was tested in triplicate to ensure accuracy and reproducibility.[13,14] The sensitive components corresponding to the 10 electronic nose sensors (W1C, W5S, W3C, W6S, W5C, W1S, W1W, W2S, W2W, and W3S) are shown in Figure S2. The response values of 10 sensors within 150 s are shown in Table S2.

2.2.2. Electronic Tongue Setup and Signal Acquisition. Approximately 1.0 g of WA and CA powder were weighed. Subsequently, 120 g of pure water was added and the mixture was stirred thoroughly. The sample was then dispersed by using ultrasonic treatment for 20 min. The suspension was transferred to a centrifuge tube and centrifuged at 4000 rpm for 5 min then cooled to room temperature. 20 mL of the supernatant was placed in a specific container and tested on a TS-5000Z Taste Analysis System (INSENT, Japan).[14,15] The sensitive components corresponding to the electronic tongue sensor are shown in Table S3. The first taste (such as sourness, saltiness, etc.) and aftertaste (such as aftertaste-bitter, aftertaste-astringency, etc.) could be obtained through an electronic tongue test.

30 mM NaCl (30 mM) and tartaric acid (0.3 mM) were mixed to make a reference solution. The output value of the reference solution was used as a tasteless point. The tasteless points of 9 sensors are shown in Supporting Information Table S4. The taste output value of the sample below the tasteless point indicates that the sample has no such taste. The Richness in the table is the aftertaste of umami, which reflects the persistence of the sample's umami. It is also known as the durability of umami. Aftertaste-bitter [aftertaste (B)] reflects the degree of residual bitterness, and aftertaste-astringency [aftertaste (A)] reflects the degree of residual astringency.

2.2.3. Electronic Eye Setup and Signal Acquisition. After the NH310+ portable computer color difference meter (Shenzhen Sanenshi Technology) was turned on and stabilized for 5 min, a whiteboard was used to correct it. The initial values were recorded as L_0, a_0, and b_0. The test began after the light was stabilized.[16−18]

Approximately 2.0 g of WA and CA powder were weighed. Subsequently, they were spread on the slide, pressed flat, and placed on the whiteboard. Each sample was tested in triplicate, and the average value was taken. 5 mm aperture, light source D65, and standard viewing angle 10° were set. L^*, a^*, and b^* values were recorded, and the ΔE value was calculated. L^* is the brightness value. The larger the value, the greater the brightness. a^* is a red-green value. The larger the value, the redder it is, while the smaller the value, the greener. b^* is the yellow-blue value. The larger the value, the yellower, while the smaller the value, the bluer. ΔE is the total chromaticity value calculated by the formula $\Delta E = [(L - L_0)^2 + (a - a_0)^2 + (b - b_0)^2]^{1/2}$.[19]

2.3. Analysis of Volatile Components of WA and CA. Volatile components are one of the main components in *A. sinensis*. *The Chinese Pharmacopoeia* (2020) stipulates that volatile components in *A. sinensis* should not be less than 0.4% (mL/g). Therefore, volatile components and their relative contents in 15 batches of WA and CA were analyzed by 7890B-7000D Gas Chromatograph Mass Spectrometer (Agilent Technologies) using the literature method with a slight modification.[20] 0.5 g WA and CA powder (0.5 g) were taken and placed in a 20 mL headspace sampling bottle. 2-Octanol at a concentration of 3 mg/L was used as the internal standard. Subsequently, a saturated NaCl solution was added. The sample was heated to 80 °C for 30 min. Then, the headspace microextraction injection needle was inserted into the headspace bottle for 30 min, and the sample was analyzed at 250 °C for 5 min. The chromatographic conditions were as follows. The chromatographic separation was achieved on an HP-5MS column (30 m × 0.25 mm × 0.25 μm, Agilent Technologies). The initial column temperature was 50 °C lasting for 2 min and then increased to 180 °C within 5 min at 5 °C/min, and continuously increased to 250 °C at 10 °C/min within 5 min. The carrier gas was helium, and the flow rate was 1.0 mL/min. The inlet temperature was 250 °C, and the transmission line temperature was 280 °C. The electron energy of the EI source was 70 eV, the ion source temperature was 230 °C, and the four-stage rod temperature was 150 °C. The shunt ratio was 50:1, and the scanning range was from m/z 40 to 600.

2.4. Quantitative Fingerprint Analysis of WA and CA. The standards, chlorogenic acid, ferulic acid, senkyunolide I, senkyunolide H, coniferyl ferulate, falcarindiol, 3-*n*-butylphthalide, senkyunolide A, ligustilide, 3-butylidenephthalide, and levistilide A, were dissolved in methanol to prepare a mixed reference solution with mass concentrations of 0.092, 0.078, 0.326, 0.303, 0.247, 0.253, 0.261, 0.178, 3.323, 0.316, and 0.059 mg/mL, respectively. 2.5 g of *A. sinensis* powder was weighed accurately and placed in a tapered bottle with a plug. 25 mL of methanol was added, and the mass was weighed. An ultrasound was conducted for 45 min. Subsequently, the tapered bottle with a plug was allowed to cool to room temperature and weighed again. Any weight loss was compensated for by adding methanol, followed by thorough shaking.[21] The extract solution was filtrated and analyzed on the LC-2030CPlus high-performance liquid chromatograph (DAD) (Shimadzu Company, Japan). Shim-pack GIST C18 chromatographic column (250 mm × 4.6 mm, 5 μm, Shimadzu Corporation, Japan) was used.

2.5. Data Analysis. Software "Origin 2022", "Simca", "Graphpad Prism", and "SPSS 25.0" were used for data analysis.

3. RESULTS AND DISCUSSION

3.1. Bionic Technology Signal Acquisition Results. Principal component analysis (PCA) is a multivariate statistical

https://doi.org/10.1021/acsomega.4c04400
ACS Omega 2024, 9, 41408−41418

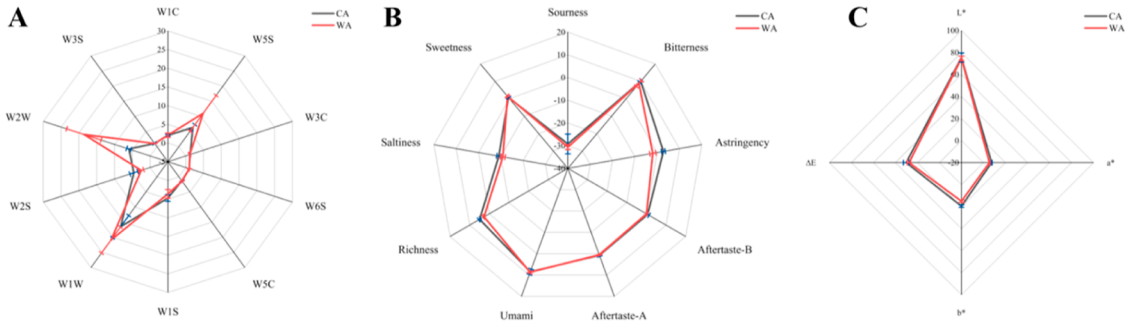

Figure 3. Radar maps of WA and CA based on electronic nose signals (A), electronic tongue signals (B), and electronic eye signals (C).

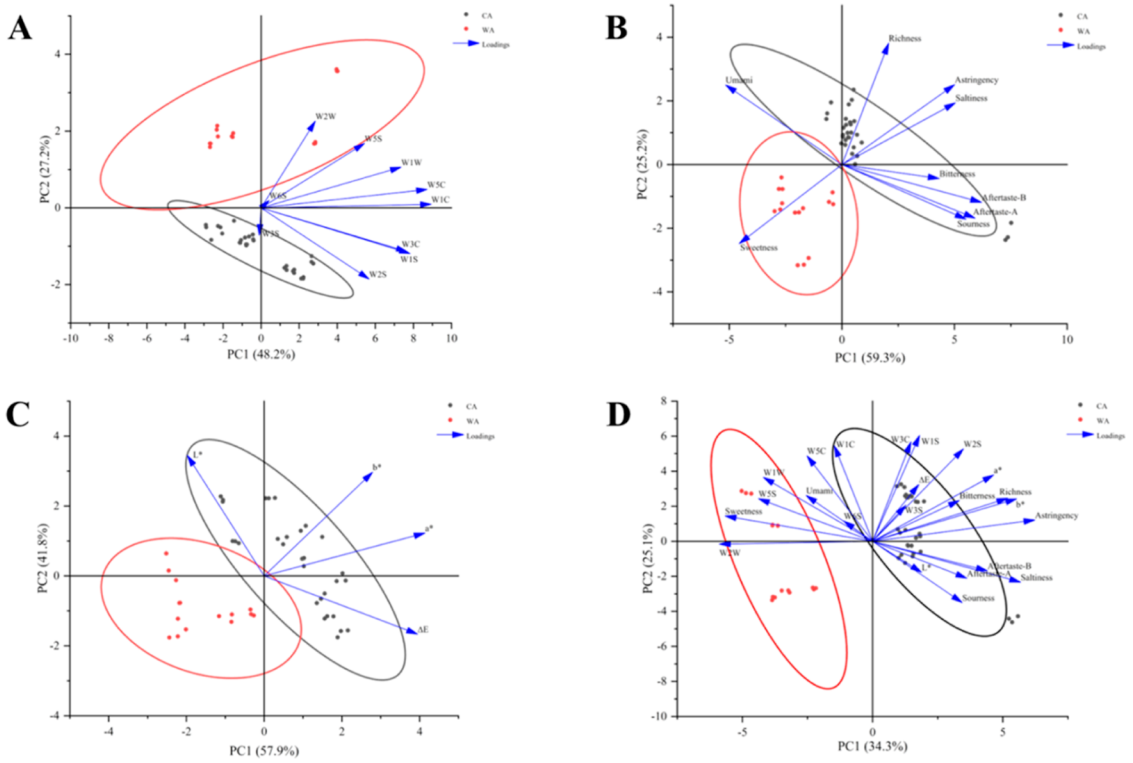

Figure 4. PCA score plots and loading plots of WA and CA based on electronic nose signals (A), electronic tongue signals (B), and electronic eye signals (C) and fusion signals (D).

method that can transform and reduce the dimensionality of the collected data. Radar maps can effectively represent multidimensional data and are very suitable for displaying performance data. The radar maps of WA and CA based on electronic nose signals, electronic tongue signals, and electronic eye signals were drawn, as displayed in Figure 3. Figure 3A shows that the difference in odor characteristics between WA and CA mainly concentrated on W2W, W2S, W1W, and W5S, namely, aromatic components/organic sulfides, alcohols, inorganic sulfides, and nitrogen oxides. Figure 3B shows that the taste characteristics of WA and CA were different. The sourness and saltiness values of WA and CA were both below the tasteless point, indicating that except for sourness and saltiness, other taste indexes were effective taste indexes of *A. sinensis*. Among them, the astringencies and richnesses of WA and CA were significantly different. The astringency of CA was stronger than that of WA, and the umami of CA was more durable than that of WA. There is no significant difference between the other taste indicators except sourness and saltiness. Figure 3C showed that there was no significant difference in L^* between WA and CA, but a^* and b^* of CA were slightly higher than those of WA, indicating that CA powder was more red and yellow than WA. As can be seen from the standard deviation in Figure 3, the electronic nose data of CA are more stable than those of WA. In addition, the standard deviation of the electronic tongue and electronic eye of WA and CA are smaller than that of the electronic nose, indicating that the electronic tongue and electronic eye data are more stable than those of electronic nose. This may be because the phthalides in *A. sinensis* are highly affected by factors such as light and temperature, which leads to the instability of the odor of *A. sinensis*.[22]

PCA score plots and loading plots are illustrated in Figure 4. Relevant studies have shown that in PCA, the PC1 accounts for a larger weight.[23] Therefore, Figure 4A−C shows that WA and CA were different in odor, taste, and color. The loading plot is to represent the influencing factors that contribute greatly to the PC1 and PC2 in the two-dimensional diagram of PCA. The closer the influence factor is to the two-dimensional coordinate of the sample, the greater the influence of the

https://doi.org/10.1021/acsomega.4c04400
ACS Omega 2024, 9, 41408−41418

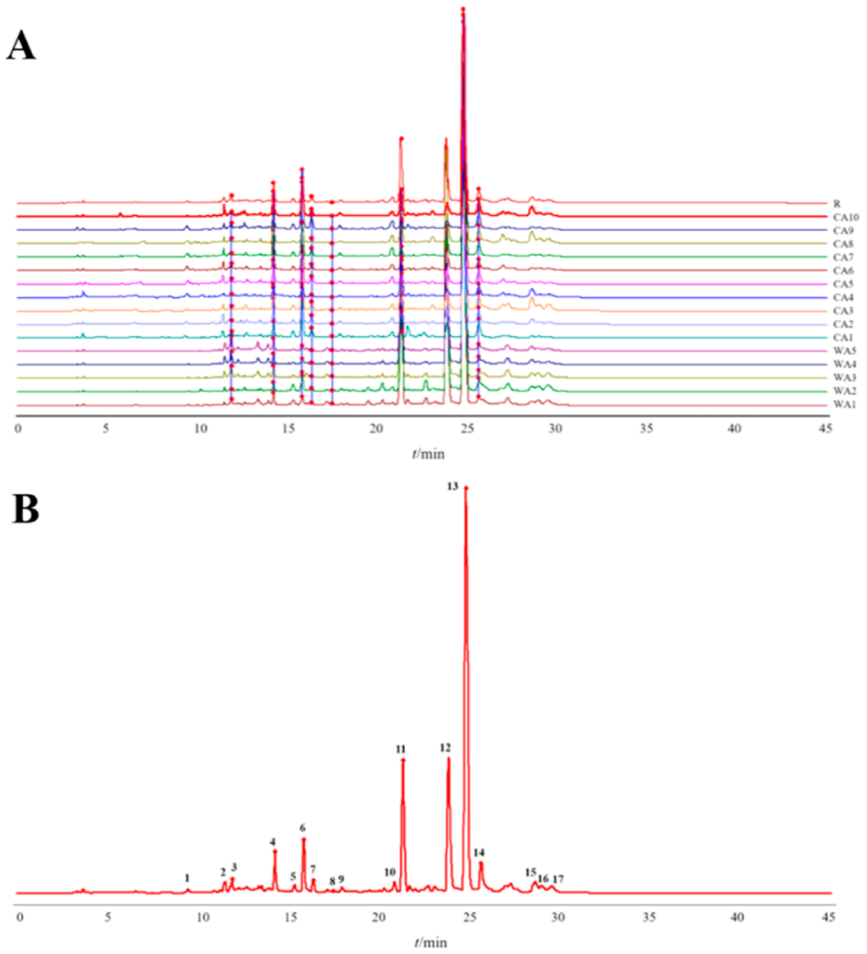

Figure 5. HPLC fingerprints of 15 batches of *A. sinensis* (A) and control fingerprints of *A. sinensis* (median method) (B).

loading factor.[24] Figure 4A shows that W2W and W5S point toward WA, and W3S and W2S point toward CA. Figure 4B shows that richness, astringency, saltiness, and bitterness point toward CA and sweetness point toward WA. In Figure 4C, L^*, a^*, b^*, and ΔE all point toward CA. The results indicate that W2W, W5S, and sweetness have a greater influence on WA. In addition, W3S, W2S, richness, astringency, saltiness, bitterness, L^*, a^*, b^*, and ΔE have a greater influence on CA.

Since the principle of PCA is to find the maximization of variance in the low dimensions, the pretreatment of original signals by setting the mean value at the origin of each variable and then dividing them by their standard deviation is not suitable. In order to eliminate the effect of index dimension, the data of the electronic nose, electronic tongue, and electronic eye were all imported to "Excel" and scaled in the range between −1 and 1 to obtain the fusion signals.[10] The PCA score plot and loading plot of WA and CA based on fusion signals are shown in Figure 4D. Compared with Figure 4A−C, there is no intersection between WA and CA regions in Figure 4D. The results show that there were significant differences between WA and CA based on fusion signals. In addition, Figure 4D shows that W3C, W1C, W2S, W3S, bitterness, richness, astringency, L^*, a^*, b^*, and ΔE have a greater effect on CA, and W1W, W5S, W2W, and sweetness have a greater effect on WA. The results are consistent with those shown in Figure 4A−C. The accuracy and feasibility of the fusion signals were further illustrated. All four sets of data were found to be within 95% confidence intervals. The parameter R^2X represents the explanatory power of the model in the X-axis direction, that is, how much percentage of information the model explains in the original data through principal components. The parameter Q^2 represents the predictive ability of the model. The closer the R^2X and Q^2 values are to 1, the more stable and reliable the model is. In general, the model can be considered valid when the Q^2 value is greater than 0.5. For the model of the electronic nose, R^2X and Q^2 were 0.955 and 0.785, respectively. The values were 0.974 and 0.867 for electronic tongue and 0.996 and 0.967 for electronic eyes. For the model of fusion signals, the values were 0.954 and 0.806. The results show that the explanatory and predictive power of the PCA models established by both single and fusion signals are good.

3.2. Analysis and Comparison of Volatile Components of WA and CA. TIC chromatograms are shown in Figures S3 and S4. The relative peak area (PA) of each component in volatile oils of WA and CA was calculated by the PA normalization method, and the compounds were identified by NIST spectral database retrieval (matching degree required to reach more than 80%). Each compound was represented by relative content (%), and the results are shown in Table S5. Volatile components of WA mainly include (*E*)−3-butylidene-4,5-dihydroisobenzofuran-1 (3*H*)-one (60.723%), *Z*-butylidenephthalide (4.133%), benzaldehyde,2,4,5-trimethyl- (1.932%), etc. There were 4 species with a content greater than 1%. Volatile components of CA mainly include (*E*)−3-butylidene-4,5-dihydroisobenzofuran-1 (3*H*)-one (50.151%),

https://doi.org/10.1021/acsomega.4c04400
ACS Omega 2024, 9, 41408−41418

(*Z*)-3-butylidene-4,5-dihydroisobenzofuran-1 (3*H*)-one (16.054%), *Z*-butylidenephthalide (7.882%), etc. There were 9 types with a content greater than 1%. WA contained 36 qualitative chemical components, while CA had 30. Both WA and CA shared 13 qualitative volatile components. Qualitative component contents of WA and CA account for 77.915 and 88.908%, respectively. The highest volatile component in WA and CA was (*E*)-3-butylidene-4,5-dihydroisobenzofuran-1(3*H*)-one. Moreover, the content of (*E*)-3-butylidene-4,5-dihydroisobenzofuran-1(3*H*)-one in WA was higher than that in CA.

3.3. Quantitative Fingerprint Analysis of WA and CA.

3.3.1. HPLC Analysis and Method Validation. In order to obtain the best separation in a relatively short period of time and to maximize the characterization of chemical components of *A. sinensis* in the fingerprints, several chromatographic conditions, including mobile phase, detection wavelength, flow rate, injection volume, and column temperature, were optimized. The final chromatographic condition was that octadecylsilane-bonded silica gel was used as a stationary phase with 0.1% acetic acid glacial solution as mobile-phase A and methanol as mobile-phase B. The flow rate was 0.8 mL/min. Gradient elution, 0−5 min, 5−18% B; 5−6.5 min, 18−35% B; 6.5−9 min, 35−55% B; 9−15 min, 55−70% B; 15−20 min, 70−80% B; 20−25 min, 80% B, 25−45 min, 80−5% B. The detection wavelength was 270 nm. The column temperature was 30 °C. Due to the small number of WA, a batch of CA samples (CA5) were randomly selected to establish a fingerprint for verification of the optimized HPLC. The precision of the instrument was evaluated by 6 consecutive injections of the same test solution. The repeatability of the method was evaluated by parallel preparation of 6 test solutions with the same method. The stability of the test solution was evaluated by analysis of the test solution at 0, 4, 8, 12, 16, and 24 h. The RSD values of retention times (RTs) and PAs of common peaks for precision (RT < 0.18%; PA < 3.14%), repeatability (RT < 2.51%; PA < 1.93%), and stability (RT < 0.69%, PA < 1.82%) were all less than 4.0%, demonstrating that the developed method was valid and reliable for fingerprint establishment.

3.3.2. Establishment and Similarity Analysis of Fingerprints. The chromatographic data of 15 batches of *A. sinensis* samples were imported into the "TCM Chromatographic Fingerprint Similarity Evaluation System" to establish the HPLC fingerprints (Figure 5A). A random batch of samples (CA10) were selected as the reference chromatogram (R), the time window was set at 0.1 min; and the control chromatogram was established using the median method. A total of 17 chromatographic peaks with good stability were obtained as common peaks (Figure 5B). A total of 8 chromatographic peaks were identified through chromatographic comparison with the mixed reference solution and literature review. Peak 3, 4, 6, 7, 8, 9, 10, 11, 13, 14, and 16 were identified as chlorogenic acid, ferulic acid, senkyunolide I, senkyunolide H, senkyunolide A, coniferyl ferulate, falcarindiol, 3-*n*-butylphthalide, senkyunolide A, ligustilide, 3-butylidenephthalide, and levistilide A, respectively.

The similarity evaluation was performed, and the results are shown in Table 1. The results showed that the similarity of 15 batches of *A. sinensis* was above 0.9. The mean similarity of WA (0.939) was slightly lower than that of CA (0.994), so there were slight differences between the WA and CA.

Table 1. Results of Similarity Evaluation

sample	similarity
WA1	0.905
WA2	0.979
WA3	0.922
WA4	0.937
WA5	0.951
CA1	0.993
CA2	0.998
CA3	0.999
CA4	0.985
CA5	0.998
CA6	0.997
CA7	0.998
CA8	0.996
CA9	0.981
CA10	1

3.3.3. Analysis of 11 Indicator Components. The contents of 11 indicator components in WA and CA were determined and employed for further cluster analysis, PCA, and partial least-squares discriminant (PLS-DA) analysis. For cluster analysis, the samples were measured by the squared Euclidean distance and zero-mean normalization. The results are shown in Figure 6A. The result showed that WA and CA could be well grouped into two categories. PCA score plot and loading plot of 11 indicator components were drawn, as shown in Figure 6B. The PC1 was 55.4%, indicating that there were differences in the content of 11 indicator components between WA and CA. The contents of senkyunolide H, senkyunolide I, falcarindiol, 3-butylidenephthalide, 3-*n*-butylphthalide, and ferulic acid had a significant impact on CA, while the contents of coniferyl ferulate, levistilide A, and ligustilide had a significant impact on WA. The histogram of content was drawn, as shown in Figure 6C. The results showed that the contents of ferulic acid, senkyunolide I, senkyunolide H, coniferyl ferulate, falcarindiol, 3-*n*-butylphthalide, and ligustilide were significantly extremely different between WA and CA. There was a significant difference in chlorogenic acid, 3-butylidenephthalide, and levistilide A contents between the two. However, there was no significant difference in the senkyunolide A content between the two.

PLS-DA is a statistical method mainly used for high-dimensional data classification and discriminant analysis, aiming to find patterns that distinguish between two or more categories. It can be used for classification and discriminant analysis. Herein, the PLS-DA model was calculated, with the content of the 11 indicator components as the independent variable (X) and the dummy matrix that codes the class belonging to the samples using binary coding as the dependent variable (Y). The values of the explanatory parameter R^2X, R^2Y, and predictive parameter Q^2 were 0.773, 0.976, and 0.956, respectively, indicating that the constructed model exhibited a reliable predictor and statistical significance. From the PLS-DA score plot presented in Figure 6D, it could be found that WA and CA could be well distinguished, which is largely consistent with the PCA analysis. In the PLS-DA model, the variable with variable importance projection (VIP) value greater than 1 is considered to be the main contributor to group classification. As shown in Figure 6E, ligustilide possessed the highest VIP value among the 11 indicator components, indicating that it is the component with the greatest difference between WA and

https://doi.org/10.1021/acsomega.4c04400
ACS Omega 2024, 9, 41408−41418

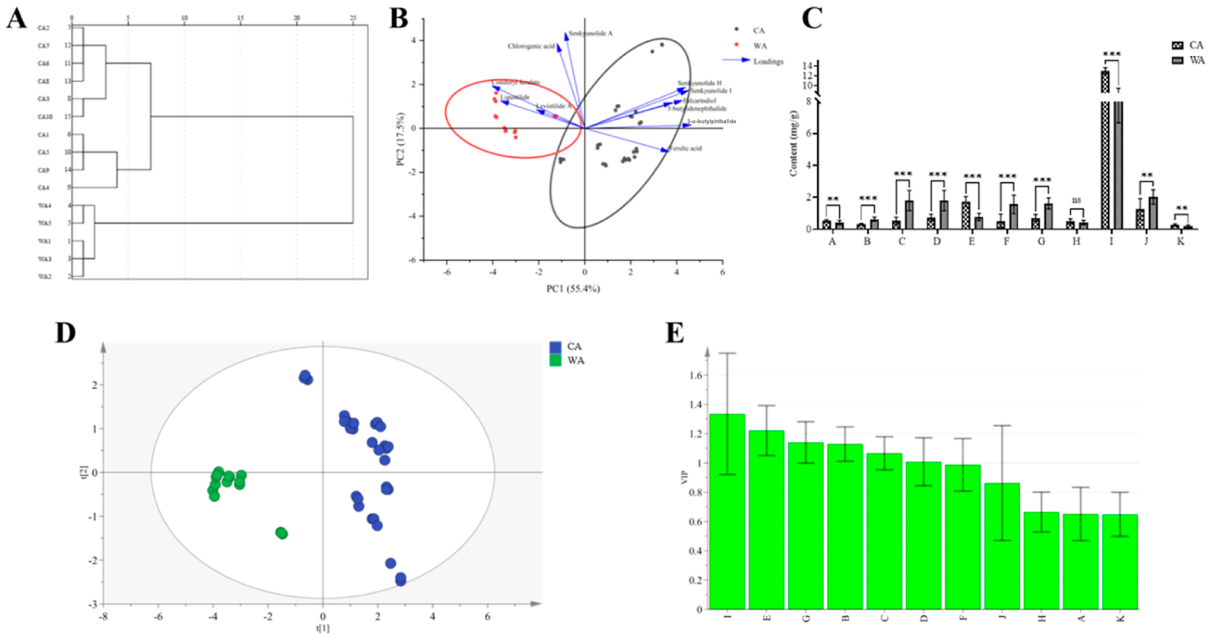

Figure 6. Clustering analysis tree of fingerprints (A), PCA (B), column chart for the content determination of 11 indicator components (C), score plot of PLS-DA model (D), and VIP value plot about 11 indicator components in the PLS-DA model (E).

CA. In addition, VIP values of coniferyl ferulate, 3-*n*-butylphthalide, ferulic acid, senkyunolide I, and senkyunolide H were all greater than 1, indicating that these compounds had the greatest difference between WA and CA. Such a result was basically consistent with that of Figure 6C.

3.3.4. Correlation Analysis between Bionic Technologies and 11 Indicator Components. Bivariate correlation analysis (Pearson correlation analysis) was adopted to conduct correlation analysis between the signals of the electronic nose, electronic tongue, and electronic eye and the contents of 11 indicator components. The results are shown in Table 2. Based on the research, the content of chlorogenic acid had a significant negative correlation with L^*, a^*, and b^*, had no significant correlation with electronic nose sensors, and had a significant negative correlation with bitterness, astringency, aftertaste-B, and saltiness. Also, the content of ferulic acid was significantly positively correlated with L^*, b^*, and ΔE, correlated considerably with W5S, W3C, W1S, W2S, and W2W, and significantly associated with astringency, umami, richness, saltiness, and sweetness. The content of senkyunolide I was significantly correlated with L^*, a^*, b^*, and ΔE and had significant correlations with W3C, W1S, W2W, and W3S, having an extremely significant correlation with bitterness, astringency, richness, and sweetness. The content of senkyunolide H had an extremely significant correlation with L^*, a^*, b^*, and ΔE, had an extremely substantial correlation with W3C, W1S, W2S, W2W, and W3S, and had a significant correlation with bitterness, astringency, richness, and sweetness. The content of coniferyl ferulate was significantly negatively associated with a^*, b^*, and ΔE and was significantly correlated with W1S, W1W, W2S, W2W, and W3S. There was an extremely significant correlation with bitterness, astringency, aftertaste-B, richness, saltiness, and sweetness. The content of falcarindiol had an extremely significant positive correlation with a^*, b^*, and ΔE^*, had an extremely substantial correlation with W1S, W2S, W3S, and W2W, and had a significant correlation with bitterness, astringency, umami, sourness, and sweetness. The content of 3-*n*-butylphthalide had an extremely significant positive correlation with a^*, b^*, and ΔE^*, had an extremely substantial correlation with W3C, W1S, W2S, W3S, and W2W, and had a significant correlation with bitterness, astringency, richness, and sweetness. The content of senkyunolide A was significantly negatively correlated with a^*. There was a significant positive correlation with W1C and W5C and a significant negative correlation with the richness. The content of ligustilide was significantly negatively correlated with a^*, b^*, and ΔE. It had a significant correlation with W5S, W3C, W5C, W1S, W1W, W2S, W2W, and W3S, and it had a significant correlation with sourness, bitterness, astringency, aftertaste-B, aftertaste-A, richness, saltiness, and sweetness. The content of 3-butylidenephthalide was extremely significantly positively correlated with a^*, b^*, and ΔE. There was a significant correlation with W1S, W2S, W2W, and W3S and an extremely significant positive correlation with bitterness, astringency, and richness. The content of levistilide A was extremely significantly associated with L^*, a^*, and ΔE, and it was extremely significantly correlated with W5S, W2W, W2S, and W3S. There was an extremely significant correlation with astringency, richness, saltiness, and sweetness. It can be seen that the odor, taste, and color of WA and CA have some correlation with the content of the indicator components.

3.4. Discussion. Environmental factors, such as temperature, light, and water availability, exert a significant influence on the morphological features of plants and the accumulation of secondary metabolites.[25] Wild TCM is subjected to more biological and abiotic stress factors during its growth. These external stresses can have adverse effects, such as variability and distortion of the root morphology. The adverse effects may lead to changes in the content or proportion of secondary metabolites, which may make wild TCM have a darker root bark color and a stronger or unique odor than cultivated products. However, the weak adversity effect leads to the delicate epidermis, lighter color, and weaker odor of cultivated TCM.[9] Related studies have found that WA has stronger resistance to adversity, disease, and insect pests, and stronger

https://doi.org/10.1021/acsomega.4c04400
ACS Omega 2024, 9, 41408−41418

Table 2. Correlation Analysis between Odor, Taste, Color, and Indicator Components of WA and CA[a]

bionic technologies	bionic technical indicators	chlorogenic acid	ferulic acid	senkyunolide I	senkyunolide H	coniferyl ferulate	falcarindiol	3-*n*-butylphthalide	senkyunolide A	ligustilide	3-butylidenephthalide	levistilideA
electronic eye	L^*	−0.321*	0.076	−0.356*	−0.427**	0.003	−0.257	−0.214	0.073	−0.024	−0.147	0.520**
	a^*	−0.318*	0.803**	0.752**	0.720**	−0.793**	0.728**	0.832**	−0.317*	−0.771**	0.609**	−0.499**
	b^*	−0.444**	0.772**	0.544**	0.476**	−0.753**	0.554**	0.688**	−0.210	−0.765**	0.503**	−0.203
	ΔE	0.041	0.424**	0.720**	0.747**	−0.516**	0.624**	0.674**	−0.252	−0.499**	0.491**	−0.692**
electronic nose	W1C	−0.135	0.117	0.157	0.208	0.052	0.158	0.198	0.350*	0.167	0.091	0.187
	W5S	−0.028	−0.478**	−0.233	−0.179	0.247	−0.095	−0.215	0.132	0.541**	0.071	0.402**
	W3C	−0.199	0.498**	0.403**	0.437**	−0.252	0.283	0.500**	0.122	−0.295*	0.153	−0.243
	W6S	−0.099	−0.179	0.101	0.139	−0.007	0.205	0.065	0.072	0.056	−0.073	−0.188
	W5C	−0.053	−0.057	−0.003	0.064	0.235	−0.009	0.031	0.395**	0.313*	−0.070	0.224
	W1S	−0.292	0.552**	0.532**	0.559**	−0.380*	0.456**	0.635**	0.116	−0.325*	0.352*	−0.155
	W1W	0.044	−0.265	−0.160	−0.075	0.447**	−0.19	−0.126	0.233	0.535**	−0.127	0.167
	W2S	−0.278	0.753**	0.660**	0.670**	−0.532**	0.519**	0.772**	−0.042	−0.572**	0.397**	−0.393**
	W2W	0.225	−0.747**	−0.605**	−0.541**	0.695**	−0.483**	−0.642**	0.266	0.843**	−0.339*	0.540**
	W3S	0.026	0.102	0.546**	0.570**	−0.377*	0.559**	0.511**	−0.086	−0.386**	0.374*	−0.498**
electronic tongue	sourness	−0.172	−0.226	−0.172	−0.239	−0.133	−0.331*	−0.187	0.119	−0.377*	−0.171	0.012
	bitterness	−0.385**	0.146	0.387**	0.344*	−0.583**	0.402**	0.397**	0.135	−0.454**	0.447**	0.051
	astringency	−0.402**	0.593**	0.688**	0.626**	−0.804**	0.587**	0.696**	−0.034	−0.857**	0.415**	−0.391**
	aftertaste-B	−0.301*	−0.057	0.064	−0.014	−0.388**	−0.043	0.055	0.139	−0.524**	0.083	−0.001
	aftertaste-A	−0.292	−0.195	−0.036	−0.105	−0.257	−0.134	−0.066	0.249	−0.380**	−0.032	0.116
	umami	0.212	0.351*	0.174	0.231	0.173	0.278	0.164	−0.120	0.294	0.006	−0.144
	richness	−0.220	0.914**	0.707**	0.663**	−0.706**	0.642**	0.808**	−0.303*	−0.780**	0.515**	−0.479**
	saltiness	−0.377*	0.324*	0.215	0.138	−0.537**	0.116	0.261	−0.194	−0.726**	−0.021	−0.386**
	sweetness	0.119	0.201	−0.402**	−0.329*	0.595**	−0.316*	−0.379*	0.162	0.792**	−0.177	0.468**

[a]Note: *$P < 0.05$; **$P < 0.01$.

https://doi.org/10.1021/acsomega.4c04400
ACS Omega 2024, 9, 41408−41418

resistance to early bolting ability.[26] Therefore, it is speculated that one of the main reasons for the differences in morphological features and chemical composition content between WA and CA is the adverse effects caused by external stress.

This study draws the following conclusions: ① Electronic nose, electronic tongue, and electronic eye can distinguish WA from CA. The taste and color of *A. sinensis* are more stable than the odor. According to Figure 4, compared with the independent signals, fusion signals can distinguish WA and CA better. ② The results of volatile component analysis combined with the results of quantitative fingerprints showed that ligustilide was the main component of *A. sinensis*, which was consistent with related literature reports.[27,28] ③ The main chemical components of WA and CA are basically the same, so it can be preliminarily judged that the alternative use of WA and CA is feasible. ④ There were differences between WA and CA in odor, taste, color, and content of indicator components. There were correlations between morphological features and the content of indicator components.

This study showed that the use of an electronic nose, electronic tongue, and electronic eye, combined with appropriate analytical methods, offers a more direct and perceptive approach to the comparative analysis of TCM. This provides a new comprehensive evaluation method for the quality detection and comparative study of TCM in the future. Since the clinical efficacy of TCM is the most convincing criterion for evaluating the quality of TCM, the author puts forward the following prospects for the comparative study of wild and cultivated TCM in the future: ① Existing studies on pharmacodynamic differences between wild and cultivated TCM mainly focus on animal models,[29−31] and occasionally cell models.[32] There were no standardized and rigorous clinical pharmacodynamic observation reports. Due to the complexity of TCM components, the small dosage of a single TCM prescription, and the differences between the mouse model and the human body, there is no significant difference in common efficacy.[33,34] As a result, the difference in drug effect is not closely related to the difference in chemical components. More sensitive and reliable animal experimental models should be further explored, and new administration methods and observation indicators should be established in order to further study the differences between the pharmacodynamic effects of wild and cultivated TCM. ② At present, comparative studies of the quality of wild and cultivated TCM mainly focus on the differences in morphological features and chemical components. There is a lack of research on the molecular mechanism of their differences, compared with cultivated plants such as crops[35−37] and fruits.[38−40] It is necessary to strengthen the research on the differences between wild and cultivated TCM in terms of genome, transcriptome, etc. Based on the differences in the content of primary and secondary metabolites and the regulatory pathways of plant hormones on germplasm variation, environmental stresses, human intervention, and other factors, relevant research on the regulatory mechanism of genes and transcriptomes of wild and cultivated TCM can be carried out to find out the reasons for the differences. It is of great significance to further develop and optimize the imitation wild cultivation technology of TCM and explore the alternative uses of wild and cultivated TCM.

■ ASSOCIATED CONTENT

Data Availability Statement

Due to the nature of this research, participants of this study did not agree for their data to be shared publicly, so Supporting Information is not available.

Supporting Information

The Supporting Information is available free of charge at https://pubs.acs.org/doi/10.1021/acsomega.4c04400.

Microscopic features of WA and CA roots, response intensity curve of electronic nose sensors, TIC chromatogram of volatile oil in WA and CA, basic information on 15 batches of WA and CA samples, sensitive components corresponding to electronic nose sensors and electronic tongue sensors, taste output values of the reference solution, and volatile components in WA and CA (PDF)

■ AUTHOR INFORMATION

Corresponding Author

Ling Jin − *College of Pharmacy, Gansu University of Chinese Medicine, Lanzhou 730000 Gansu, China*; Email: zyxyjl@163.com

Authors

Yiyang Chen − *College of Pharmacy, Gansu University of Chinese Medicine, Lanzhou 730000 Gansu, China*; orcid.org/0009-0007-2513-4266

Jialing Zhang − *College of Pharmacy, Gansu University of Chinese Medicine, Lanzhou 730000 Gansu, China*

Juanjuan Liu − *College of Pharmacy, Gansu University of Chinese Medicine, Lanzhou 730000 Gansu, China*

Huifang Hu − *College of Pharmacy, Gansu University of Chinese Medicine, Lanzhou 730000 Gansu, China*

Liangcai Wang − *College of Pharmacy, Gansu University of Chinese Medicine, Lanzhou 730000 Gansu, China*

Complete contact information is available at: https://pubs.acs.org/10.1021/acsomega.4c04400

Author Contributions

Y.C: data curation, formal analysis, visualization, validation, methodology, investigation, conceptualization, and writing—original draft, review, and editing; J.Z: supervision, conceptualization, and writing—review and editing; J.L: methodology and writing—review and editing; H.H: investigation, resources, and writing—review and editing; L.W: supervision and writing—review and editing; LJ: supervision, project administration, funding acquisition, conceptualization, and writing—review and editing. All authors have read and agreed to the published version of the manuscript.

Notes

The authors declare no competing financial interest.

■ ACKNOWLEDGMENTS

This study was supported by the Gansu Provincial Science and Technology Major Project (23ZDFA013-1), Strategic Research and Consulting Project of the Chinese Academy of Engineering (GS2021ZDA06-2), Gansu Provincial Department of Education "Double First-Class" Key Scientific Research Project (GSSYLXM-05), Gansu Provincial University Youth Doctoral Fund funded project (2023QB-094), and

Gansu Provincial Science and Technology Project (20JR5RA182).

REFERENCES

(1) Meng, X.; Yu, P.; He, L.; Guan, Y. Discussion on past, present and future of traditional Chinese medicine resources based on social development level. *Chin. Tradit. Herb. Drugs* **2022**, *53* (16), 5235−5244.
(2) Wang, F.; Chen, S.; Liu, Y.; Chen, H.; Hu, Y.; Li, S.; Chen, L. Advances and Prospects of Chinese Herbal Medicine Planting Industry in China. *Modern Chin. Med.* **2023**, *25* (6), 1163−1171.
(3) Lan, X.; Tian, C.; Zhan, Z.; Zhou, L.; Li, X.; Qiu, Z.; Nan, T.; Yuan, Q.; Lin, X.; Tian, C.; Chen, M.; Kang, L. Comparison of Wild and Cultivated Codonopsis pilosula Based on Traditional Quality Evaluation. *Chin. J. Exp. Tradit. Med. Formulae*, 1−10..
(4) Tian, C.; Hu, Q.; Zhan, Z.; Lan, X.; Li, X.; Zhou, L.; Nan, T.; Qiu, Z.; Kang, L. Comparison of Wild and Cultivated Paeoniae Radix Rubra Based on Traditional Quality Evaluation. *Chin. J. Exp. Tradit. Med. Formulae*, 1−12..
(5) Chen, L.; Wang, L.; Shu, G.; Li, J. Antihypertensive Potential of Plant Foods: Research Progress and Prospect of Plant-Derived Angiotensin-Converting Enzyme Inhibition Compounds. *J. Agric. Food Chem.* **2021**, *69* (18), 5297−5305.
(6) Zhao, K. J.; Dong, T. T. X.; Tu, P. F.; Song, Z. H.; Lo, C. K.; Tsim, K. W. K. Molecular Genetic and Chemical Assessment of Radix Angelica (Danggui) in China. *J. Agric. Food Chem.* **2003**, *51* (9), 2576−2583.
(7) Zhang, S.; He, L.; Han, L.; Yang, W.; Liu, L. Study on Wild Angelica Resources. *Modern Chin. Med.* **2012**, *14* (4), 33−36.
(8) Yan, H.; Zhang, X.; Zhu, S.; Qian, D.; Guo, L.; Huang, L.; Duan, J. Production regionalization study of Chinese angelica based on MaxEnt model. *China J. Chin. Mater. Med.* **2016**, *41* (17), 3139−3147.
(9) Wang, Y.; Yuan, C.; Qian, J.; Wang, Y.; Liu, Y.; Liu, Y.; Nan, T.; Kang, L.; Zhan, Z.; Guo, L.; Huang, L. Reviews and Recommendations in Comparative Studies on Quality of Wild and Cultivated Chinese Crude Drugs. *Chin. J. Exp. Tradit. Med. Formulae* **2024**, *30*, 1−20.
(10) Xu, M.; Wang, J.; Zhu, L. The Qualitative and Quantitative Assessment of Tea Quality Based on E-Nose, E-Tongue and E-Eye Combined with Chemometrics. *Food Chem.* **2019**, *289*, 482−489.
(11) Li, C.; Wan, H.; Wu, X.; Yin, J.; Zhu, L.; Chen, H.; Song, X.; Han, L.; Yang, W.; Yu, H.; Li, Z. Discrimination and Characterization of the Volatile Organic Compounds in Schizonepetae Spica from Six Regions of China Using HS-GC-IMS and HS-SPME-GC-MS. *Molecules* **2022**, *27* (14), 4393.
(12) Zhang, C.; Zheng, X.; Ni, H.; Li, P.; Li, H. Discovery of Quality Control Markers from Traditional Chinese Medicines by Fingerprint-Efficacy Modeling: Current Status and Future Perspectives. *J. Pharm. Biomed. Anal.* **2018**, *159*, 296−304.
(13) Yang, W.; Zhang, S.; He, L.; Wang, W. Analysis on the odor of Radix Angelica Sinensis based on electronic nose. *J. Tradit. Chin. Vet. Med.* **2014**, *33* (4), 50−52.
(14) Wang, R.; Guo, W.; Liu, Q.; Xia, C. The odor characteristics of aster were analyzed based on electronic nose and electronic tongue. *Chin. Tradit. Pat. Med.* **2022**, *44* (5), 1693−1697.
(15) Zhou, X.; Yang, S.; Xu, M.; Wan, J. Discrimination of Coptis chinensis Franch and its processed products by electronic tongue. *Chin. Tradit. Pat. Med.* **2015**, *37* (9), 1993−1997.
(16) Zhang, X.; Wu, H.; Yu, X.; Lu, Y.; Luo, H.; Yang, H.; Xu, M.; Guo, R.; Li, Z.; Tang, L.; Wang, Z. Quality Evaluation of Andrographis Herba Based On Electronic-eye Technique. *Chin. J. Exp. Tradit. Med. Formulae* **2019**, *25* (1), 189−195.
(17) Zhen, Z.; Wang, Y.; Wei, H.; Cui, W.; Li, H.; Zhang, X. Quality standard and processing technology of stir-fried yam with bran based on color change. *Chin. Tradit. Pat. Med.* **2021**, *43* (3), 816−819.
(18) Duan, J.; Xiao, Y.; Liu, Y.; Song, H.; Dou, Z. Optimization of steaming time of Cornus officinalis by QAMS combined with electronic-eye and electronic-tongue techniques. *Chin. Tradit. Herb. Drugs* **2017**, *48* (6), 1108−1116.
(19) Xie, Y.; Ye, X.; Zhang, J.; Huang, M.; Zhang, T.; Wan, Q.; Liu, Y.; Liu, M.; Yi, H.; Kang, A. Based on color quantification and HS-GC-MS, the composition and color changes of Paeonia alba before and after processing were discussed. *Lishizhen Med. Mater. Med. Res.* **2022**, *33* (10), 2418−2421.
(20) Wang, S.; Yu, A.; Yan, X.; Zheng, H.; Chen, Q.; Xie, Q.; Wang, L. Analysis of Volatilis Components Changes Before and After Combination in Angelica and Ligusticum by Headspace Solid Phase Microextraction Gas Chromatography Mass Spectrometry. *Chin. Arch. Tradit. Chin.* **2020**, *38* (5), 118−124.
(21) Zhang, M.; Zhu, T.; Jin, L.; Wang, F.; Xu, L.; Kang, S. Quality differences of different origins and varieties of Angelicae sinensis based on HPLC multi-index composition determination and multi-pattern recognition method of fingerprint. *Chin. Tradit. Herb. Drugs* **2022**, *53* (19), 6187−6199.
(22) Yang, Y.; Feng, Y.; Chen, J.; Xu, M. Research advance in phthalides and their biological activities. *Nat. Prod. Res. Dev.* **2022**, *34* (8), 1439−1453.
(23) Dong, W.; Hu, R.; Long, Y.; Li, H.; Zhang, Y.; Zhu, K.; Chu, Z. Comparative Evaluation of the Volatile Profiles and Taste Properties of Roasted Coffee Beans as Affected by Drying Method and Detected by Electronic Nose, Electronic Tongue, and HS-SPME-GC-MS. *Food Chem.* **2019**, *272*, 723−731.
(24) Hu, J.; He, L.; Wang, L.; Qiao, M.; Lu, D.; Chen, P.; Deng, J.; Yi, Y. Evaluation of Sichuan Style Similar Complex Flavors (Fish Flavor, Litchi Flavor and Sweet and Sour Flavor) Based on Partial Specific Sensor Electronic Tongue and Heracles II Electronic Nose. *Food Sci. Technol.* **2021**, *46* (8), 244−250.
(25) Zhu, T.; Zhang, M.; Su, H.; Li, M.; Wang, Y.; Jin, L.; Li, M. Integrated Metabolomic and Transcriptomic Analysis Reveals Differential Mechanism of Flavonoid Biosynthesis in Two Cultivars of Angelica Sinensis. *Molecules* **2022**, *27* (1), 306.
(26) Feng, W.; Liu, P.; Yan, H.; Yu, G.; Guo, Z.; Zhu, L.; Ma, J.; Qian, D.; Duan, J. Transcriptomic data analyses of wild and cultivated Angelica sinensis root by high-throughput sequencing technology. *China J. Chin. Mater. Med.* **2020**, *45* (8), 1879−1886.
(27) Wang, S.; Shen, X.; Meng, Y.; Yan, X.; Yan, W.; Yu, A.; Zheng, H.; Wang, L. Analysis of volatile oil in common components of Angelica medicinal parts by HS-SPME-CS-MS. *Chin. J. Hosp. Pharm.* **2019**, *39* (5), 433−438.
(28) Yang, J.; Liu, T.; Yan, H.; Zhang, X.; Peng, M.; Xia, X. Extraction and Analysis of Main Components Angelica Essential Oil Based on the Combination of SFE and GC-MS Technique. *Guide of China Med.* **2014**, *12* (23), 2−3.
(29) Li, Y.; Lin, Z.; Teng, J.; Wang, C.; Zhuang, X.; Zhao, J.; Wang, Y.; Lv, G.; Lin, H. Comparison of Pharmacodynamics between Wild and Cultivated Kushen (Sophora flavescens) Based on Traditional Efficacy. *Pharmacol. Clin. Chin. Mater. Med.* **2022**, *38* (1), 130−134.
(30) Liu, M.; Lu, J.; Lin, Z.; Li, W.; Zhang, W.; Huang, X.; Lv, G. A comparative study on the pharmacodynamics of wild and cultivated asaroxin based on traditional efficacy. *Ginseng Res.* **2023**, *35* (6), 18−22.
(31) Ma, J.; Man, Q.; Yan, X.; Deng, Y.; Yang, Z.; Yang, X. Detoxification of hepatotoxicity caused by wild and cultivated licorice in strychnine. *Chin. Tradit. Pat. Med.* **2023**, *45* (8), 2718−2722.
(32) Mohsin, M.; Negi, P.; Ahmed, Z. Determination of the Antioxidant Activity and Polyphenol Contents of Wild Lingzhi or Reishi Medicinal Mushroom, Ganoderma Lucidum (W.Curt. Fr.) P. Karst. (Higher Basidiomycetes) from Central Himalayan Hills of India. *Int. J. Med. Mushrooms* **2011**, *13* (6), 535−544.
(33) Li, Y.; Li, F.; Tong, L.; Wen, S.; Wei, Q.; Ren, S. Comparative investigation on pharmacodynamics of wild and planting Gentiana. *J. Chin. High Alt. Med. Biol.* **2006**, No. 4, 254−258.
(34) Donghai, Z.; Fu, M.; Yang, Q.; Fang, J.; Song, H.; Yang, B.; Xiong, Y. Pharmacological research of wild and cultivated Atractylodes lancea. *China J. Chin. Mater. Med.* **2010**, *35* (13), 1758−1762.

https://doi.org/10.1021/acsomega.4c04400
ACS Omega 2024, 9, 41408−41418

(35) Veremeichik, G. N.; Grigorchuk, V. P.; Butovets, E. S.; Lukyanchuk, L. M.; Brodovskaya, E. V.; Bulgakov, D. V.; Bulgakov, V. P. Isoflavonoid Biosynthesis in Cultivated and Wild Soybeans Grown in the Field under Adverse Climate Conditions. *Food Chem.* **2021**, *342*, 128292.
(36) Zhang, H.; Jiang, H.; Hu, Z.; Song, Q.; An, Y.-Q. C. Development of a Versatile Resource for Post-Genomic Research through Consolidating and Characterizing 1500 Diverse Wild and Cultivated Soybean Genomes. *BMC Genomics* **2022**, *23* (1), 250.
(37) Duan, Y.; Duan, S.; Xu, J.; Zheng, J.; Hu, J.; Li, X.; Li, B.; Li, G.; Jin, L. Late Blight Resistance Evaluation and Genome-Wide Assessment of Genetic Diversity in Wild and Cultivated Potato Species. *Front. Plant Sci.* **2021**, *12*, 710468.
(38) Wang, P.; Yang, Y.; Shi, H.; Wang, Y.; Ren, F. Small RNA and Degradome Deep Sequencing Reveal Respective Roles of Cold-Related microRNAs across Chinese Wild Grapevine and Cultivated Grapevine. *BMC Genomics* **2019**, *20* (1), 740.
(39) Wang, L.; He, F.; Huang, Y.; He, J.; Yang, S.; Zeng, J.; Deng, C.; Jiang, X.; Fang, Y.; Wen, S.; Xu, R.; Yu, H.; Yang, X.; Zhong, G.; Chen, C.; Yan, X.; Zhou, C.; Zhang, H.; Xie, Z.; Larkin, R. M.; Deng, X.; Xu, Q. Genome of Wild Mandarin and Domestication History of Mandarin. *Mol. Plant* **2018**, *11* (8), 1024−1037.
(40) Jing, D.; Liu, X.; He, Q.; Dang, J.; Hu, R.; Xia, Y.; Wu, D.; Wang, S.; Zhang, Y.; Xia, Q.; Zhang, C.; Yu, Y.; Guo, Q.; Liang, G. Genome Assembly of Wild Loquat (Eriobotrya Japonica) and Resequencing Provide New Insights into the Genomic Evolution and Fruit Domestication in Loquat. *Hortic. Res.* **2023**, *10* (2), uhac265.

https://doi.org/10.1021/acsomega.4c04400
ACS Omega 2024, 9, 41408−41418